

Entanglement and absorbing-state transitions in interactive quantum dynamicsNicholas O’Dea ¹, Alan Morningstar ¹, Sarang Gopalakrishnan,² and Vedika Khemani¹¹*Department of Physics, Stanford University, Stanford, California 94305, USA*²*Department of Electrical Engineering, Princeton University, Princeton, New Jersey 08544, USA*

(Received 9 January 2023; accepted 3 January 2024; published 31 January 2024)

Nascent quantum computers motivate the exploration of quantum many-body systems in nontraditional scenarios. For example, it has become natural to explore the dynamics of systems evolving under both unitary evolution and measurement. Such systems can undergo dynamical phase transitions in the entanglement properties of quantum trajectories *conditional* on the measurement outcomes. Here, we explore dynamics in which one attempts to (locally) use those measurement outcomes to steer the system toward a target state, and we study the resulting phase diagram as a function of the measurement and feedback rates. Steering succeeds when the measurement and feedback rates exceed a threshold, yielding an absorbing-state transition in the trajectory-averaged density matrix. We argue that the absorbing-state transition generally occurs at different critical parameters from the entanglement transition in individual trajectories and has distinct critical properties. The efficacy of steering depends on the nature of the target state: in particular, for local dynamics targeting long-range correlated states, steering is necessarily slow and the entanglement and steering transitions are well separated in parameter space.

DOI: [10.1103/PhysRevB.109.L020304](https://doi.org/10.1103/PhysRevB.109.L020304)

Introduction. Phases and criticality in quantum many-body dynamics are topics of fundamental interest. For unitary dynamics, various questions have been explored, such as the growth of entanglement [1–3], the emergence of hydrodynamics [4–6], or the effects of disorder [7–9]. Recently, motivated by advances in quantum computing hardware, “monitored” quantum systems subject to repeated local measurements have also come under intense investigation [10,11]. These systems were shown to display the surprising phenomenon of entanglement phase transitions as a function of measurement rate [12–20]. Such phase transitions are only visible in the properties of *individual* quantum trajectories [21] corresponding to specific sequences of measurement outcomes, so they bear a prohibitive postselection cost that is exponential in the space-time volume (with exceptions in Clifford dynamics [22,23], space-time dual dynamics [24–26], or replacing measurements with swaps into an environment [27]). Monitored dynamics can be enriched by using the measurement outcomes, say, for adaptively controlling the subsequent dynamics [28–34]. Error correction is one example of such *interactive quantum dynamics* with a transition as a function of the error rate [35]. Understanding novel dynamical phenomena in interactive evolution is an active area of inquiry, especially topical in light of experimental advances in building devices capable of quantum control via measurements and feedback.

In this work, we consider interactive quantum dynamics with unitary evolution and measurements, where the measurement outcomes are used to apply local unitaries that *steer* the system towards target states [36–38]. The target states are absorbing states, so that the dynamics can evolve to the target state, but cannot leave it. We discuss steering both to trivial product states and to entangled symmetry-protected topological (SPT) states. Our dynamics

only uses local feedback (in contrast to nonlocal classical communication); i.e., each feedback operation depends only on the measurement immediately preceding it at the same location. Therefore, the average density matrix dynamics is described by a time-independent local quantum channel. Unlike the quantum channels that occur in the standard (non-adaptive) measurement-induced transition, our channel is *not* unital, so its steady state need not be the maximally mixed state. The channels we consider can, in fact, undergo an absorbing-state phase transition [39–46] separating an “absorbing phase” in which a pure zero-entropy target state is reached in a time at most polynomial in system size, from an “active phase” in which it is not.

We study interactive quantum dynamics as a function of the measurement rate p_m and the fraction of measurements that are followed by feedback, p_f . This yields a phase diagram with two transitions: an entanglement phase transition in individual trajectories, driven by p_m , and an absorbing-state transition in the average density matrix, driven by the total rate of feedback events $p_m p_f$ (Fig. 1). We provide numerical evidence and analytical arguments that these do not coincide in general. When we target a trivial polarized product state and use maximally efficient feedback, $p_f = 1$, the transitions occur at sufficiently close p_m that we cannot numerically distinguish the locations of the critical points. Nevertheless, we find that quantities associated with the trajectory-averaged density matrix scale with directed-percolation critical exponents that are completely different from the exponents associated with the entanglement transition in individual trajectories. This finding is natural if one posits two separate transitions, but implies a drastic violation of one-parameter scaling otherwise.

Errors above a target state with short-range correlations can be locally corrected, allowing for efficient local feed-

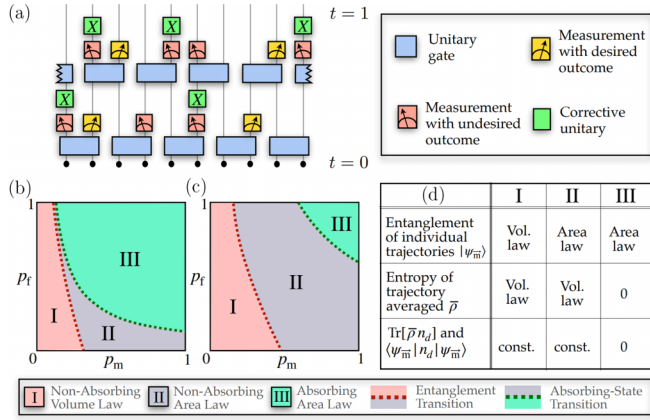


FIG. 1. Monitored quantum circuits with feedback and schematic depictions of their associated phase diagrams. (a) A quantum circuit model with $|\uparrow\uparrow\cdots\uparrow\rangle$ as its target state (see text). Sketch of the phase diagrams for interactive dynamics targeting (b) the all-up state and (c) an SPT cluster state. The two phase boundaries are close or widely separated near $p_f = 1$ in panels (b) and (c), respectively. The absorbing-state phase transition curves in panels (b) and (c) satisfy $p_m p_f = \text{const.}$ (d) A table of the properties of the three phases.

back. For target states with long-range correlations, such as a ferromagnet or a topologically ordered state, error correction requires pairing up domain walls or anyons over long distances, which requires long-range classical communication [47–49]. Absent such communication, the error correction dynamics is described by a local quantum channel, which has a light cone. Steering from a product state to a long-range correlated state therefore takes a time that diverges with system size, even at $p_m = p_f = 1$ where all trajectories are area-law entangled. To explore these consequences of locality, we study dynamics targeting an SPT state using both symmetric and symmetry-breaking operations. In the former case, but not the latter, the entanglement and absorbing-state transitions are well separated, consistent with the logic above.

Polarized absorbing state. We first consider a spin-1/2 model with the target state $|\psi_t\rangle = |\uparrow\uparrow\uparrow\cdots\uparrow\rangle$. The model comprises two-site nearest-neighbor unitary gates applied in a brickwork fashion in a one-dimensional system of length L with periodic boundary conditions. Each gate is block diagonal and locally leaves the $|\uparrow\uparrow\rangle$ state invariant, but acts as a Haar-random unitary $U(3)$ in the 3×3 block of states spanned by $\{|\uparrow\downarrow\rangle, |\downarrow\uparrow\rangle, |\downarrow\downarrow\rangle\}$. The unitary dynamics leaves $|\psi_t\rangle$ invariant, but is otherwise chaotic. Each gate in the circuit is sampled independently. Unless otherwise stated, we always begin with the system in the $|\downarrow\downarrow\cdots\downarrow\rangle$ state. In between the unitary layers, we measure the Pauli Z_i operator on each site with the probability p_m . If the outcome is $+1$, locally corresponding to the $|\uparrow\rangle_i$ state, we do nothing. If the outcome is -1 , a corrective unitary X_i is applied with the probability p_f to steer the system towards $|\psi_t\rangle$ [Fig. 1(a)]. As a channel, this measure-and-correct operation is equivalent to a qubit reset, which is accessible on current hardware [46]. A given quantum trajectory, $|\psi_{\vec{m}}(t)\rangle$, is labeled by the sequence of measurement outcomes, \vec{m} , encountered at each position until time t ; the label also implicitly includes the action of

feedback events conditioned on the outcomes. We denote the density matrix obtained by averaging over trajectories, feedback events, and choices of random circuits as $\bar{\rho}$.

We describe the phase diagram of this model in Fig. 1 using properties of trajectories and properties of $\bar{\rho}$ at times linear in system size. When the total rate of feedback operations $p_m p_f$ exceeds the critical value $p_c \approx 0.1$, $\bar{\rho}$ approaches the absorbing state (phase III). Here, every trajectory approaches the same unentangled target state. When $p_m p_f < p_c$, $\bar{\rho}$ remains mixed up to times exponential in L . However, individual trajectories exhibit two phases, even at $p_f = 0$: a volume-law phase (phase I) and an area-law phase (phase II). In phase II, each trajectory stays active and visits *different* area-law states, so $\bar{\rho}$ remains high-entropy. We argue below that phase II intervenes between phases I and III, even when $p_f = 1$.

Absorbing state transition. The absorbing-state transition is visible in $\bar{\rho}$ and observable via conventional expectation values. In Ref. [50], we show that the diagonal elements of $\bar{\rho}$ evolve under the transfer matrix of a classical stochastic process, while the off-diagonal elements vanish after one complete time step. This mapping gives us access to much larger system sizes and allows us to convincingly demonstrate that this absorbing-state transition is in the directed percolation universality class. In the classical process, the effect of the averaged measurements is to locally send \downarrow to \uparrow with the probability $p_m p_f$, while the effect of the averaged unitaries is to mix the local configurations $\uparrow\downarrow$, $\downarrow\uparrow$, and $\uparrow\uparrow$ with equal probability $1/3$ [50]. Note that the averaged dynamics are now described by only a single parameter $p \equiv p_m p_f$ describing the total rate of measurements with feedback. This stochastic process has an all-up absorbing state and undergoes an absorbing-state transition characterized by the behavior of “defects”, i.e., down spins. The density of defects

$$n_d = \frac{1}{L} \sum_i \frac{1 - Z_i}{2}$$

serves as an order parameter that rapidly approaches zero (exponentially in time) in the absorbing phase, but reaches a long-lived nonzero value in the nonabsorbing phase (for times exponential in L). In Fig. 2(a), we see that the density of defects is nonzero below $p_c \approx 0.1$ and vanishes above p_c . The curve $p_m p_f = p_c \approx 0.1$ defines the absorbing-state critical line depicted in Fig. 1(c). Note that a nonzero n_d implies an extensive entropy for $\bar{\rho}$, with the entropy density being maximal at $n_d = 0.5$ and decreasing as p_c is approached.

For a classical stochastic process with a single absorbing state, a nondisordered transfer matrix, and no additional symmetries, the critical properties are expected to be in the directed percolation (DP) universality class. We confirm this expectation in Figs. 2(b) and 2(c), using techniques discussed in Ref. [51]. We expect that n_d satisfies the following critical scaling:

$$n_d(t, L) \sim t^{-\delta} \Phi\left((p - p_c)t^{1/\nu_{\parallel}}, \frac{t^{1/z}}{L}\right). \quad (1)$$

where $\nu_{\parallel} = z\nu_{\perp}$ and z is the dynamical scaling exponent. To probe the values of δ and p_c , we define a time-dependent estimate $\delta(t)$ so that $n_d(t) \sim 1/t^{\delta(t)}$, and we extract $\delta(t)$ from the quantity $\log_{10}[n_d(t)/n_d(10t)]$. We expect that at the crit-

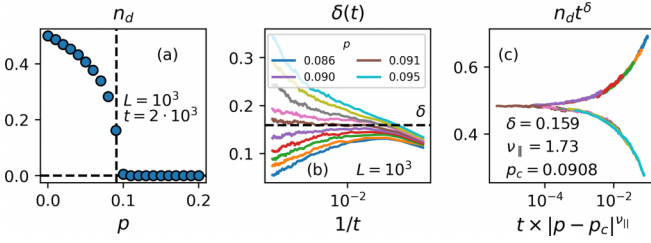


FIG. 2. Absorbing-state phase transition. (a) The sample-averaged defect density n_d as a function of $p = p_m p_f$. Between 10^3 and 2×10^3 samples were averaged for each data point shown. Values were computed via the mapping to a classical stochastic model and initialized with random bitstrings. (b) The running estimate of the critical exponent δ as a function of inverse time $1/t$. The critical p_c is estimated to be the value of p for which the curve remains constant as $1/t \rightarrow 0$, and an estimate for δ is that constant value. (c) Scaling collapse of n_d data to the form of Eq. (1). The critical exponents are those of directed percolation.

ical point, and for $t^{1/z}/L$ sufficiently small, $\delta(t)$ is constant, while it vanishes in the nonabsorbing phase and diverges in the absorbing phase. Figure 2(b) shows a value of δ consistent with directed percolation's $\delta_{DP} = 0.159$ and a critical probability of $p_c = 0.09085(5)$. We see scaling collapse of these curves in Fig. 2(c) using this p_c and δ_{DP} and $\nu_{DP||} = 1.73$. Thus, as anticipated, our model's absorbing-state transition falls under the directed percolation universality class.

Entanglement phase transition. We now locate and characterize the entanglement phase transition via exact simulations of quantum trajectories for $L \leq 24$. We first consider the cut $p_f = p_m$ through the phase diagram in Fig. 1(c); the feedback along this cut is weak enough that the entanglement phase transition is numerically well separated from the absorbing-state transition. We benchmark the entanglement transition against previous analyses of models without feedback. We use the tripartite quantum mutual information $I_3 = S_{Q_1} + S_{Q_2} + S_{Q_3} - S_{Q_1 \cup Q_2} - S_{Q_2 \cup Q_3} - S_{Q_3 \cup Q_1} + S_{Q_1 \cup Q_2 \cup Q_3}$, which was argued to be constant at the critical point and show a crossing [15,52]. Here S_A is the von Neumann entanglement entropy of subsystem A , and Q_n is the n th contiguous quarter of the system. We evaluate I_3 at $t = 2L$, anticipating that the entanglement transition will have the dynamical exponent $z = 1$ [17,18,53]. The crossing of I_3 yields the critical point $p_m^c = p_f^c \cong 0.130(5)$, which is well-separated from the absorbing-state phase transition at $p_m = p_f = \sqrt{p_c} \cong \sqrt{0.09085} = 0.3014$ found above (Fig. 2). We perform a scaling collapse near the critical point, and the critical exponent $\nu \cong 1.1(2)$ obtained is consistent with previous estimates of ν for the entanglement transition in monitored circuits with Haar-random gates [52]. With this estimate of p_m^c , we verify [50] that the dynamics at p_m^c are consistent with the exponent $z = 1$ by examining the purification of an initial mixed state [15,32,54]. Thus, along the line $p_f = p_m$, the entanglement and absorbing-state transitions are well separated, and the former displays the same critical properties as monitored circuits without feedback.

We now consider the case of full-strength feedback and vary p_m while $p_f = 1$ is fixed. In this case, every measurement-and-feedback operation leaves the spin in the $|\uparrow\rangle$ state; hence,

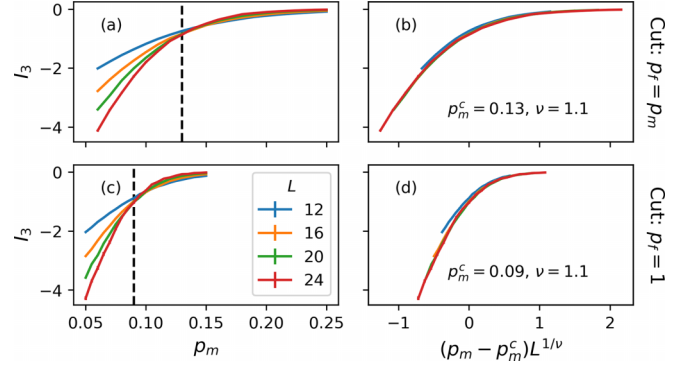


FIG. 3. Tripartite quantum mutual information. The data are averaged over $5 \times 10^2 - 5 \times 10^3$ circuit realizations and quantum trajectories in simulations of full wave-function evolution, and over times $t = 2L$ and $2L + \frac{1}{2}$ to avoid even-odd effects. The top row corresponds to the cut $p_f = p_m$, and the bottom to $p_f = 1$. Vertical dashed lines mark estimates of the critical points: $p_m^c \cong 0.130(5)$ (a) and $p_m^c \cong 0.090(5)$ (c). Panels (b) and (d) show the finite-size scaling collapse of the form $I_3 = f[(p_m - p_m^c)L^{1/\nu}]$, with $\nu \cong 1.1(2)$.

measurements not only drive trajectories to low-entanglement states, but also specifically towards the polarized state. As a result, the entanglement and absorbing-state transitions come closer together and a similar analysis of I_3 locates the entanglement transition at $p_m^c \cong 0.090(5)$ [see Fig. 3(c)], numerically indistinguishable from the location of the absorbing-state transition found above (Fig. 2). A natural question is then whether the two phase transitions coalesce as $p_f \rightarrow 1$, or remain distinct critical phenomena. In order to see that the two transitions remain distinct, we determine their dynamical exponents z [55]. We extract z for the entanglement transition using the purification setup [50]—which examines the entropy S of a system initially in a mixture of two random orthogonal states—and for the absorbing-state transition using the density of defects n_d . In Fig. 4 we show both S and n_d data for times $t \gtrsim L^z$. The entropy continues to scale like $S \sim f(t/L)$, i.e., $z = 1.0(1)$, and n_d scales according to $\delta = 0.16(8)$ and $z = 1.6(1)$ corresponding to directed percolation. The picture that emerges is one in which the two

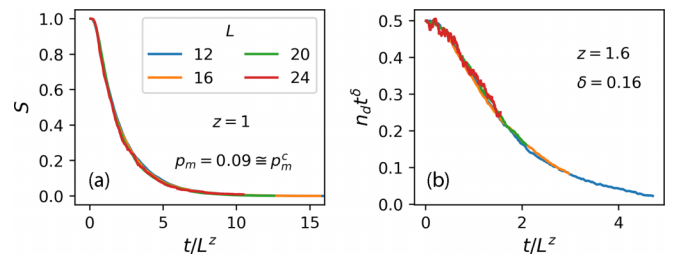


FIG. 4. Dynamical critical scaling along $p_f = 1$. The system is initialized in a mixed state with 1 bit of entropy as described in the Supplemental Material [50]. Data points are averages of $2 \times 10^2 - 5 \times 10^3$ samples. (a) The second Rényi entropy of the density matrix S vs scaled time. Data collapse is consistent with the scaling form $S = f(t/L)$. (b) The scaled density of defects vs scaled time. Data collapse is consistent with $n_d = t^{-\delta} \Phi(0, t/L^z)$ at the critical point [Eq. (1)]. The z values are not consistent in panels (a) and (b), indicating distinct critical phenomena.

phase transitions can become close in p_m at strong feedback ($p_f = 1$); however, they remain distinct critical phenomena that happen on parametrically different timescales as indicated by the different z values.

Argument for separate transitions. We now argue more directly that a sliver of phase II generically separates the two transitions, provided that the absorbing-state transition is continuous. We perform a Stinespring dilation [35] of the channel at $p_f = 1$, such that each measurement consists of swapping out one of the system spins for an ancilla spin prepared in $|\uparrow\rangle$. The steady-state entropy of $\bar{\rho}$ is the entanglement between the system and ancilla qubits; meanwhile, the entanglement entropy of trajectories is that of the system's wave function once we measure all the ancillas. Consider the dynamics when $n_d \ll 1$. “Live” (spin- \downarrow) regions are dilute, and collisions between them are rare. However, processes where a qubit in the live region is swapped into the environment are common, since p_m is $O(1)$. Suppose the live region is initially entangled with the rest of the system. Before it encounters a neighbor, it undergoes many measurement-and-feedback processes. Therefore, the rest of the system is now entangled with the live region together with the qubits that were swapped out. Collisions are rare, so the number of swapped-out qubits exceeds the number of qubits that remain in the live region. By the decoupling principle [56], the live region is decoupled from the rest of the system: instead, the rest of the system is now entangled with the environment. Since decoupling happens between collisions, large-scale entanglement cannot build up and the system remains in an area-law phase. Crucially, the rate of collisions (set by n_d) can be made arbitrarily small relative to the rate of swaps (set by p_m), by going near the absorbing-state transition [57].

SPT absorbing state. In principle, the approach described above can be generalized to steer a system to any pure state that is the unique state annihilated by a set of projectors. However, the efficacy of such steering depends on the nature of correlations in the target state: as noted in the introduction, local quantum channels have light cones and cannot prepare states with long-range correlations in finite time starting from a product state. Feedback operations targeting states with long-range correlations are inherently less efficient, since they generically move defects instead of eliminating them. One might expect, therefore, that the entanglement and absorbing-state transitions should be well separated for such target states even at $p_f = 1$.

We have tested this intuition for dynamics targeting the cluster state (ground state of $H = -\sum_i Z_i X_{i+1} Z_{i+2}$), which is an SPT state; under unitary dynamics, this state can be prepared in $O(1)$ depth if the protecting $Z_2 \times Z_2$ symmetry (that is a product of X_i on even and odd sites) is broken, while it requires depth $O(L)$ in the presence of the symmetry. An appealing feature of the cluster state is that it allows steering protocols of two types: (a) those in which the feedback completely breaks the protecting symmetry, allowing individual defects to be annihilated, and (b) those in which the feedback respects a parity symmetry that constrains defects to be annihilated in pairs. The details of the interactive dynamics are described in Ref. [50]; the results can be summarized as follows. In case (a), the phase diagram and dynamics

closely resemble the product-state example, while case (b) has the following salient differences. First, the entanglement and absorbing-state transitions are widely separated even for $p_f = 1$ [Fig. 1(d)]. Second, the absorbing-state transition belongs to the “parity-conserving” universality class [50]. Even in the absorbing phase, the approach to steady state takes a time that scales as L^2 because of the diffusion-limited recombination of defects. This conclusion does not rely on SPT symmetry, and we expect it to generalize to other models involving pairwise annihilation of defects, including in higher-dimensional systems with more exotic anyonic defects. Third, in the area-law nonabsorbing regime, individual trajectories possess a “spin-glass” SPT order [19,58,59], but the average over measurement outcomes washes out this order. Finally, with the parity symmetry, if we allow nonlocal communication so defects can be paired up more efficiently, directed-percolation universality is restored.

Discussion. In this work we explored the dynamics of single trajectories and the trajectory-averaged density matrix for a family of interactive quantum circuits with measurements and feedback. We found distinct phase transitions for single-trajectory and trajectory-averaged quantities and argued that, in general, these transitions should belong to distinct universality classes and occur at distinct critical measurement rates. The feedback allowed in our setup was based on *local* information about the state; thus, it was much more restrictive than the feedback in classical-communication-assisted protocols or in quantum error correction. An interesting direction for future work is to explore the consequences of relaxing this locality constraint and allowing for general forms of interactive dynamics that cannot be captured by local quantum channels (and therefore obey weaker locality constraints). It would also be interesting to understand cases where the two transitions may coincide [31], and the relevance of feedback to these transitions in an RG sense.

Note added. Recently, we became aware of a related work which appeared on the arXiv and was subsequently published as Ref. [60]. Our results agree where they overlap.

Acknowledgments. We are grateful to Tibor Rakovszky for many insightful discussions and close collaboration. We also thank Sebastian Diehl for discussing his work with us and Yaodong Li and David Huse for helpful discussions. This work was supported by the U.S. Department of Energy, Office of Science, Basic Energy Sciences, under Early Career Award No. DE-SC0021111 (N.O.D. and V.K.). V.K. also acknowledges support from the Alfred P. Sloan Foundation through a Sloan Research Fellowship and the Packard Foundation through a Packard Fellowship in Science and Engineering. S.G. acknowledges support from the NSF under Grant No. DMR-1653271. A.M. is supported in part by the Stanford Q-FARM Bloch Postdoctoral Fellowship in Quantum Science and Engineering and the Gordon and Betty Moore Foundations EPiQS Initiative through Grant No. GBMF8686. Numerical simulations were performed on Stanford Research Computing Center's Sherlock cluster. We acknowledge the hospitality of the Kavli Institute for Theoretical Physics at the University of California, Santa Barbara (supported by National Science Foundation Grant No. NSF PHY-1748958).

- [1] P. Calabrese and J. Cardy, Evolution of entanglement entropy in one-dimensional systems, *J. Stat. Mech.: Theory Exp.* (2005) P04010.
- [2] H. Kim and D. A. Huse, Ballistic spreading of entanglement in a diffusive nonintegrable system, *Phys. Rev. Lett.* **111**, 127205 (2013).
- [3] A. Nahum, J. Ruhman, S. Vijay, and J. Haah, Quantum entanglement growth under random unitary dynamics, *Phys. Rev. X* **7**, 031016 (2017).
- [4] V. Khemani, A. Vishwanath, and D. A. Huse, Operator spreading and the emergence of dissipative hydrodynamics under unitary evolution with conservation laws, *Phys. Rev. X* **8**, 031057 (2018).
- [5] T. Rakovszky, F. Pollmann, and C. W. von Keyserlingk, Diffusive hydrodynamics of out-of-time-ordered correlators with charge conservation, *Phys. Rev. X* **8**, 031058 (2018).
- [6] P. T. Brown, D. Mitra, E. Guardado-Sanchez, R. Nourafkan, A. Reymbaut, C.-D. Hébert, S. Bergeron, A.-M. S. Tremblay, J. Kokalj, D. A. Huse, P. Schauf, and W. S. Bakr, Bad metallic transport in a cold atom Fermi-Hubbard system, *Science* **363**, 379 (2019).
- [7] R. Nandkishore and D. A. Huse, Many-body localization and thermalization in quantum statistical mechanics, *Annu. Rev. Condens. Matter Phys.* **6**, 15 (2015).
- [8] D. A. Abanin, E. Altman, I. Bloch, and M. Serbyn, Colloquium: Many-body localization, thermalization, and entanglement, *Rev. Mod. Phys.* **91**, 021001 (2019).
- [9] F. Alet and N. Laflorencie, Many-body localization: An introduction and selected topics, *C. R. Phys.* **19**, 498 (2018).
- [10] A. C. Potter and R. Vasseur, Entanglement dynamics in hybrid quantum circuits, in *Entanglement in Spin Chains: From Theory to Quantum Technology Applications*, edited by A. Bayat, S. Bose, and H. Johannesson (Springer, Cham, 2022), pp. 211–249.
- [11] M. P. A. Fisher, V. Khemani, A. Nahum, and S. Vijay, Random quantum circuits, *Annu. Rev. Condens. Matter Phys.* **14**, 335 (2023).
- [12] Y. Li, X. Chen, and M. P. A. Fisher, Quantum Zeno effect and the many-body entanglement transition, *Phys. Rev. B* **98**, 205136 (2018).
- [13] B. Skinner, J. Ruhman, and A. Nahum, Measurement-induced phase transitions in the dynamics of entanglement, *Phys. Rev. X* **9**, 031009 (2019).
- [14] S. Choi, Y. Bao, X.-L. Qi, and E. Altman, Quantum error correction in scrambling dynamics and measurement-induced phase transition, *Phys. Rev. Lett.* **125**, 030505 (2020).
- [15] M. J. Gullans and D. A. Huse, Dynamical purification phase transition induced by quantum measurements, *Phys. Rev. X* **10**, 041020 (2020).
- [16] Y. Bao, S. Choi, and E. Altman, Theory of the phase transition in random unitary circuits with measurements, *Phys. Rev. B* **101**, 104301 (2020).
- [17] Y. Li, X. Chen, and M. P. A. Fisher, Measurement-driven entanglement transition in hybrid quantum circuits, *Phys. Rev. B* **100**, 134306 (2019).
- [18] C.-M. Jian, Y.-Z. You, R. Vasseur, and A. W. W. Ludwig, Measurement-induced criticality in random quantum circuits, *Phys. Rev. B* **101**, 104302 (2020).
- [19] M. Ippoliti, M. J. Gullans, S. Gopalakrishnan, D. A. Huse, and V. Khemani, Entanglement phase transitions in measurement-only dynamics, *Phys. Rev. X* **11**, 011030 (2021).
- [20] U. Agrawal, A. Zabalo, K. Chen, J. H. Wilson, A. C. Potter, J. H. Pixley, S. Gopalakrishnan, and R. Vasseur, Entanglement and charge-sharpening transitions in U(1) symmetric monitored quantum circuits, *Phys. Rev. X* **12**, 041002 (2022).
- [21] M. B. Plenio and P. L. Knight, The quantum-jump approach to dissipative dynamics in quantum optics, *Rev. Mod. Phys.* **70**, 101 (1998).
- [22] C. Noel, P. Niroula, D. Zhu, A. Risinger, L. Egan, D. Biswas, M. Cetina, A. V. Gorshkov, M. J. Gullans, D. A. Huse, and C. Monroe, Measurement-induced quantum phases realized in a trapped-ion quantum computer, *Nat. Phys.* **18**, 760 (2022).
- [23] Y. Li, Y. Zou, P. Glorioso, E. Altman, and M. P. A. Fisher, Cross entropy benchmark for measurement-induced phase transitions, *Phys. Rev. Lett.* **130**, 220404 (2023).
- [24] M. Ippoliti and V. Khemani, Postselection-free entanglement dynamics via spacetime duality, *Phys. Rev. Lett.* **126**, 060501 (2021).
- [25] M. Ippoliti, T. Rakovszky, and V. Khemani, Fractal, logarithmic, and volume-law entangled nonthermal steady states via spacetime duality, *Phys. Rev. X* **12**, 011045 (2022).
- [26] T.-C. Lu and T. Grover, Spacetime duality between localization transitions and measurement-induced transitions, *PRX Quantum* **2**, 040319 (2021).
- [27] Z. Weinstein, S. P. Kelly, J. Marino, and E. Altman, Scrambling transition in a radiative random unitary circuit, *Phys. Rev. Lett.* **131**, 220404 (2023).
- [28] P. Sierant, G. Chiriacò, F. M. Surace, S. Sharma, X. Turkeshi, M. Dalmonte, R. Fazio, and G. Pagano, Dissipative Floquet dynamics: From steady state to measurement induced criticality in trapped-ion chains, *Quantum* **6**, 638 (2022).
- [29] S. Wu and Z. Cai, Spontaneous symmetry breaking and localization in nonequilibrium steady states of interactive quantum systems, *Sci. bullet.* **68**, 2010 (2023).
- [30] S. J. Garratt, Z. Weinstein, and E. Altman, Measurements conspire nonlocally to restructure critical quantum states, *Phys. Rev. X* **13**, 021026 (2023).
- [31] M. Buchhold, T. Mueller, and S. Diehl, Revealing measurement-induced phase transitions by pre-selection, [arXiv:2208.10506](https://arxiv.org/abs/2208.10506).
- [32] T. Iadecola, S. Ganeshan, J. H. Pixley, and J. H. Wilson, Measurement and feedback driven entanglement transition in the probabilistic control of chaos, *Phys. Rev. Lett.* **131**, 060403 (2023).
- [33] M. McGinley, S. Roy, and S. A. Parameswaran, Absolutely stable spatiotemporal order in noisy quantum systems, *Phys. Rev. Lett.* **129**, 090404 (2022).
- [34] A. J. Friedman, O. Hart, and R. Nandkishore, Measurement-induced phases of matter require feedback, *PRX Quantum* **4**, 040309 (2023).
- [35] M. A. Nielsen and I. L. Chuang, *Quantum Computation and Quantum Information*, 10th anniversary ed. (Cambridge University, Cambridge, England, 2010).
- [36] S. Roy, J. T. Chalker, I. V. Gornyi, and Y. Gefen, Measurement-induced steering of quantum systems, *Phys. Rev. Res.* **2**, 033347 (2020).
- [37] B. Kraus, H. P. Büchler, S. Diehl, A. Kantian, A. Micheli, and P. Zoller, Preparation of entangled states

- by quantum Markov processes, *Phys. Rev. A* **78**, 042307 (2008).
- [38] L. Zhou, S. Choi, and M. D. Lukin, Symmetry-protected dissipative preparation of matrix product states, *Phys. Rev. A* **104**, 032418 (2021).
- [39] H. Hinrichsen, Non-equilibrium critical phenomena and phase transitions into absorbing states, *Adv. Phys.* **49**, 815 (2000).
- [40] M. Henkel, H. Hinrichsen, and S. Lübeck, *Non-Equilibrium Phase Transitions, Volume 1: Absorbing Phase Transitions*, Theoretical and Mathematical Physics (Springer, Dordrecht, The Netherlands, 2008).
- [41] M. Marcuzzi, M. Buchhold, S. Diehl, and I. Lesanovsky, Absorbing state phase transition with competing quantum and classical fluctuations, *Phys. Rev. Lett.* **116**, 245701 (2016).
- [42] M. Buchhold and S. Diehl, Background field functional renormalization group for absorbing state phase transitions, *Phys. Rev. E* **94**, 012138 (2016).
- [43] R. Gutiérrez, C. Simonelli, M. Archimi, F. Castellucci, E. Arimondo, D. Ciampini, M. Marcuzzi, I. Lesanovsky, and O. Morsch, Experimental signatures of an absorbing-state phase transition in an open driven many-body quantum system, *Phys. Rev. A* **96**, 041602(R) (2017).
- [44] I. Lesanovsky, K. Macieszczak, and J. P. Garrahan, Non-equilibrium absorbing state phase transitions in discrete-time quantum cellular automaton dynamics on spin lattices, *Quantum Sci. Technol.* **4**, 02LT02 (2019).
- [45] F. Carollo, E. Gillman, H. Weimer, and I. Lesanovsky, Critical behavior of the quantum contact process in one dimension, *Phys. Rev. Lett.* **123**, 100604 (2019).
- [46] E. Chertkov, Z. Cheng, A. C. Potter, S. Gopalakrishnan, T. M. Gatterman, J. A. Gerber, K. Gilmore, D. Gresh, A. Hall, A. Hankin *et al.*, Characterizing a non-equilibrium phase transition on a quantum computer, *Nat. Phys.* **19**, 1799 (2023).
- [47] L. Piroli, G. Styliaris, and J. I. Cirac, Quantum circuits assisted by local operations and classical communication: Transformations and phases of matter, *Phys. Rev. Lett.* **127**, 220503 (2021).
- [48] T.-C. Lu, L. A. Lessa, I. H. Kim, and T. H. Hsieh, Measurement as a shortcut to long-range entangled quantum matter, *PRX Quantum* **3**, 040337 (2022).
- [49] N. Tantivasadakarn, A. Vishwanath, and R. Verresen, A hierarchy of topological order from finite-depth unitaries, measurement and feedforward, *PRX Quantum* **4**, 020339 (2023).
- [50] See Supplemental Material at <http://link.aps.org/supplemental/10.1103/PhysRevB.109.L020304> for our classical mappings, purification setup for z , and our parity-conserving model's description and numerics.
- [51] J. R. G. Mendonça, Monte Carlo investigation of the critical behavior of Stavskaya's probabilistic cellular automaton, *Phys. Rev. E* **83**, 012102 (2011).
- [52] A. Zabalo, M. J. Gullans, J. H. Wilson, S. Gopalakrishnan, D. A. Huse, and J. H. Pixley, Critical properties of the measurement-induced transition in random quantum circuits, *Phys. Rev. B* **101**, 060301(R) (2020).
- [53] Y. Li, X. Chen, A. W. W. Ludwig, and M. P. A. Fisher, Conformal invariance and quantum nonlocality in critical hybrid circuits, *Phys. Rev. B* **104**, 104305 (2021).
- [54] M. J. Gullans and D. A. Huse, Scalable probes of measurement-induced criticality, *Phys. Rev. Lett.* **125**, 070606 (2020).
- [55] While the I_3 data along $p_f = 1$ still collapses well with $\nu \cong 1.1(2)$ [Fig. 3(d)], this value of ν is also consistent with the value $\nu_{\perp} = 1.1$ for directed percolation and thus the absorbing-state transition.
- [56] B. Schumacher and M. D. Westmoreland, Approximate quantum error correction, *Quantum Inf. Process.* **1**, 5 (2002).
- [57] In our numerics, n_d at the critical point is still relatively high at the accessible system sizes, so this asymptotic separation might not be visible.
- [58] A. Lavasani, Y. Alavirad, and M. Barkeshli, Measurement-induced topological entanglement transitions in symmetric random quantum circuits, *Nat. Phys.* **17**, 342 (2021).
- [59] S. Sang and T. H. Hsieh, Measurement-protected quantum phases, *Phys. Rev. Res.* **3**, 023200 (2021).
- [60] V. Ravindranath, Y. Han, Z.-C. Yang, and X. Chen, Entanglement steering in adaptive circuits with feedback, *Phys. Rev. B* **108**, L041103 (2023).